

Statistical and Machine Learning Technique to Detect and Classify Shunt Faults in a UPFC Compensated Transmission Line

Bhupendra Kumar¹, Anamika Yadav^{2*}

1- Department of Electrical Engineering, National Institute of Technology, Raipur, India.
Email: bsahare@gmail.com

2- Department of Electrical Engineering, National Institute of Technology, Raipur, India.
Email: ayadav.ele@nitrr.ac.in(Corresponding author)

Received: June 2018

Revised: September 2018

Accepted: February 2019

ABSTRACT:

In this paper, machine learning technique is used to detect and classify all shunt faults in a UPFC compensated transmission line. A four-bus three-machine system with detailed modelling of UPFC has been used for fault simulation studies in MATLAB/Simulink. Instantaneous voltage and current signals obtained at local bus terminal are processed with DFT and statistical method for feature extraction. The input features of the ANN are minimised by using the statistical method. Generated features are used for training the ANN module. Trained ANN modules are used for testing different fault conditions in the time domain. Rigorous simulation studies have been performed with a wide variety of different possible fault situations. Simulation results bring out the superiority of the scheme. Moreover, the error introduced due to CT, CCVT and Dynamic behaviour of the UPFC has been considered for testing the trained ANNs by varying the different operating mode of UPFC, and different compensation levels, wherein all the cases, the performance is found reliable.

KEYWORDS: ANN, Fault Classification, Fault Detection, FACTS, SSSC, STATCOM, Transmission Line Protection, UPFC.

1. INTRODUCTION

In modern World, energy requirement has been fulfilled by increasing power generating capacity or by increasing the power transfer capability of the existing transmission line. Advancement in the power electronic equipment technologies and automatic electronic control systems evolve the Flexible AC Transmission System (FACTS) technology. Unified power flow controller (UPFC) holds specific identity over the different FACTS devices as the ability to control real and reactive power flows as well as bus voltage magnitude simultaneously among the transmission network [1]. Establishment of those systems is either manually operated or automatically. However, during fault conditions response of these FACTS devices affects the different functional characteristics of the conventional distance relays [2-8]. UPFC is a combination of series and shunt FACTS devices known as, static synchronous series compensator (SSSC) and static synchronous compensator (STATCOM). Both compensators are connected with the common dc link. UPFC have the different operating mode, these modes of operation are achieved with the variation of operating modes of both series and

shunt converters. However, the most useful and advantageous operating mode of UPFC is Automatic Power Flow Control Mode (APFCM) [9]. Moreover, in such automatic control action, relaying end measuring signals are affected at the relaying location. The dynamic variations in the relaying measuring signals and equal compensation on per phase basis of UPFC could be the cause of relay mal-operation.

Deployment of UPFC into the transmission network would negatively influence the performance of the conventional methods, as well as, the nonlinear and dynamic behavior of VSCs makes it a challenging task [2-8]. In these regards, soft-computing based different algorithms have been proposed for the protection of UPFC compensated transmission line in last decade, which is suitable for the nonlinear and complex problem. A variety of machine learning and soft computing techniques have been presented in the last decade for fault analysis in FACTS compensated transmission line such as adaptive trip boundary for distance relaying has been proposed by using ANN in [10], and fault zone identification and classification by using decision tree (DT) [11]. DT and SVM have been utilised compara-

tively for fault zone identification in [12], SVM based distance relay zone setting in [13], DT and fuzzy rule-based differential protection scheme in [14] which requires to transmit and synchronise the measured data of both the terminal by means of communication medium. Extreme learning machine based adaptive reach setting only for the phase to ground fault is proposed in [15]. Fast discrete orthonormal S-Transforms (FDOST) for fault zone and fault loop status supervision in [16]. In [10-16] different feature extraction technique, using digital filtering has been used for the training and then testing the respective algorithms, which increases the computational burden. Moreover, in most of the cases, the dynamic behavior of UPFC during a different mode of operation and compensation levels has not been analysed. Application of Artificial Neural Network (ANN) in power system studies has been applied successfully such as fault directional estimation and fault location technique in [17], Fault detection, zone identification and fault classification in [18] for the uncompensated transmission line.

In this paper, application of ANN is presented to detect and classify shunt faults in FACTS compensated transmission line. Instantaneous voltage and current signals at relaying location are pre-processed using DFT and statistical method to reduce the feature data size for training data and the computational burden. The proposed ANN-based algorithm have been examined extensively with the simulated time domain voltage and current signals. The reliability of the proposed scheme is not affected by the variation of fault location, fault resistance, and fault inception angle. Fault detection and classification accuracy are being unaffected during error introduced in voltage and current signals due to instrument transformer such as CT and CCVT. Moreover, the sensitivity of the proposed scheme is unaltered during different mode and compensation level of UPFC.

2. SAMPLE SYSTEM

To demonstrate ANN based algorithms to detect and classify shunts faults a four buses 500 kV, 60 Hz, UPFC compensated power system network is considered as illustrated in Fig. 1. In this paper, detailed model of the UPFC controller is utilised in the sample system. The detail parameters of the transmission line and UPFC are given in [6]. The UPFC is considered between bus 1 and bus 2, to control the power flow between bus 2 and bus 3. The UPFC consists of two Voltage Source Converters (VSC), which are connected to a common dc link. Based on the control system of UPFC, the shunt connected VSC will generally operate in automatic voltage regulating mode and series connected VSC will typically be in Automatic Power Flow Control Mode (APFCM) [9]. In this paper, initially, the UPFC is considered to be in an APFCM, "The natural

power flow toward bus 2 when zero voltage is generated by the series converter (zero voltage on converter side of the four converter transformers) is $P=+870$ MW and $Q=-60$ MVar. Both the magnitude and phase angle of the series injected voltage can be varied, thus allowing control of P and Q. The UPFC controllable region is obtained by keeping the injected voltage to its maximum value (0.1 pu) and varying its phase angle from zero to 360° [19]". Although the series converter has the capability to inject voltage into the line, thereby affecting the line current and its ability for limiting the flow of line current is limited by the maximum injected voltage capability.

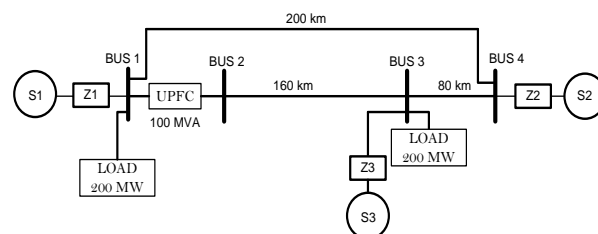


Fig. 1. One-line diagram of a simulated system.

3. PROPOSED FAULT DETECTION AND CLASSIFICATION ALGORITHM

ANN has been proven its applicability for different online and offline power system analysis and fault studies. In this scheme, Block diagram of the proposed algorithm is shown in Fig. 2. The fault detector consists of a first single ANN module for all types of shunt faults. The ANN has been trained such that, the output of the fault detector is 1 for fault situations else 0 for no fault situation. Moreover, second ANN module has been taken for all 10 types of shunt fault classification. Classifier module gives four outputs, from which, three outputs represent the three individual phases involved and one output represents ground involvement. Based on the type of fault in the protected section of the transmission line, classifier shows any one of the fault types out of 10 types of shunt fault as shown in Fig. 2. There are two ANNs that have been trained, one for fault detection and the second one is for fault classification. The architecture for each ANNs is considered such that it consists of 6 inputs, and two hidden layers occupied with 30 neurones each. Output neurone is 1 in the case of fault detection and 4 in the case of fault classification. Each ANNs are trained with Levenberg Marquardt algorithm with a high level of performance goal of $1.0e^{-07}$ and transfer function used in all the layers are tangent sigmoid.

3.1. Feature Extraction

To obtain the various possible faults simulated voltage and current signals, power system network model

is simulated in MATLAB/Simulink environment using SimPower system toolbox [19]. For the feature extraction, purpose three-phase voltage and current signals

are measured at the local terminal (bus 1 as shown in Fig.1), full cycle DFT is used for pre-processing the

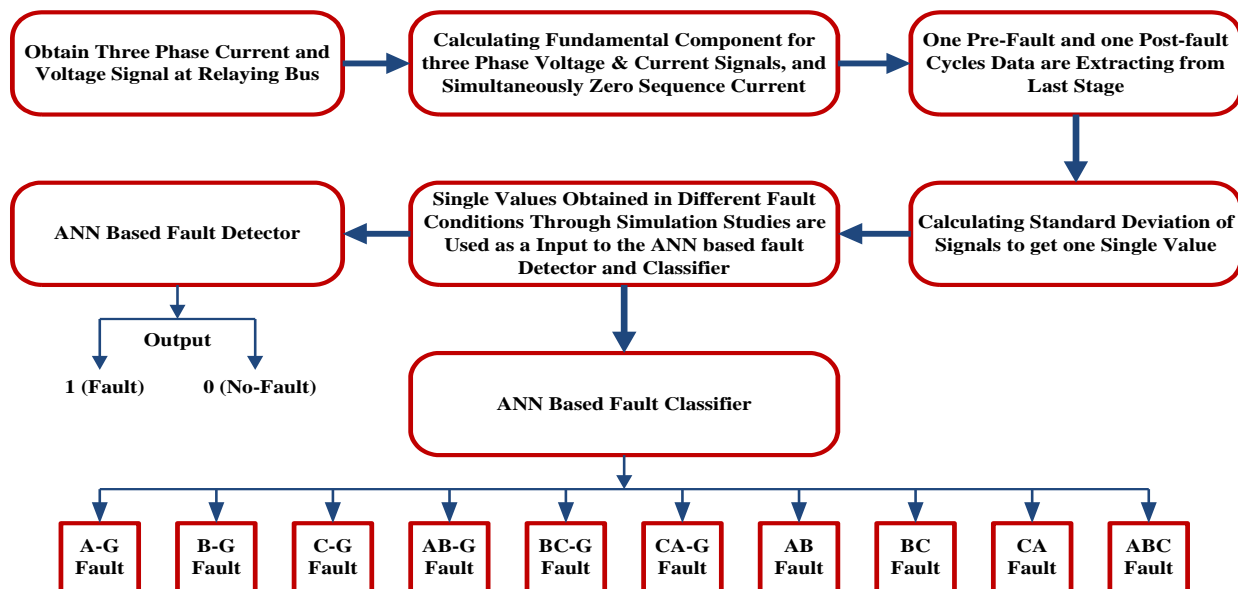


Fig. 2. Block diagram of the proposed algorithm

Instantaneous signals to obtain the fundamental component of the signals. One pre-fault and one post-fault cycle data have been extracted from the obtained fundamental component of voltage and current signals, simultaneously zero sequence current signal is calculated and one cycle pre-fault and post-fault samples are extracted. To reduce the training data sample or increase the comparable difference between normal or faulted signals, a standard deviation of the two fundamental frequency cycle data has been taken. However, 7 input (six samples for three-phase voltage and current signal and one sample for zero sequence current signal) samples have been obtained for a single faulted situation. Input data matrix has been generated for several possible faults. Simulation studies have been done with different fault parameters variations. These data matrices have been used to train the two neural networks, one for fault detection and one for fault classification. The training data for both networks is same, but it only differs from the target matrix. ANN for fault detection has one neuron, whereas, the ANN fault classification module has 4 neurons. In the target matrix, The sampling frequency of the system is 1.2 kHz during data processing. Table 1 shows the different conditions for which training data set have been generated. The large size of data is generated (4700 cases) to cover all the possible fault conditions in the sample power system. To evaluate the performance of trained ANN to detect and classify the faults in the time domain, input patterns are generated in the time domain as depicted in Fig. 3. For an example, one instantaneous current sig-

nal has been taken to show the complete process of the feature extraction. A single phase to a ground fault has been initiated at 0.255s (sample number 306) as illustrated in Fig. 3 (a). Further full cycle DFT is applied to input signal, which calculate the fundamental component of the current signal as depicted in Fig. 3 (b). Standard deviation of One cycle pre-fault and one cycle post-fault samples (total 40 samples = 2 cycles) has been calculated in a recursive manner over a sliding window of window length 40 samples (2 cycles) as illustrated in Fig. 3(c). Finally obtained standard deviated values as shown in Fig. 3 (d) has been processed to test the trained ANNs

Table 1. System parameter for training set.

Parameter	Values
Fault Type	LG [AG, BG, CG]
	LLG [ABG, BCG, CAG]
	LL[AB, BC, CA]
	LLL[ABC, ABCG]
Fault Inception Angle [Degree]	0, 45, 90, 135
Fault Resistance [Ohm]	0, 50, 100
Fault Location [km]	1- 4 (by step of 1) 5-155 (by step of 5)
UPFC References P[MW],Q[MVAr], V [p.u.]	P = 870; Q = -60; V = 1.05

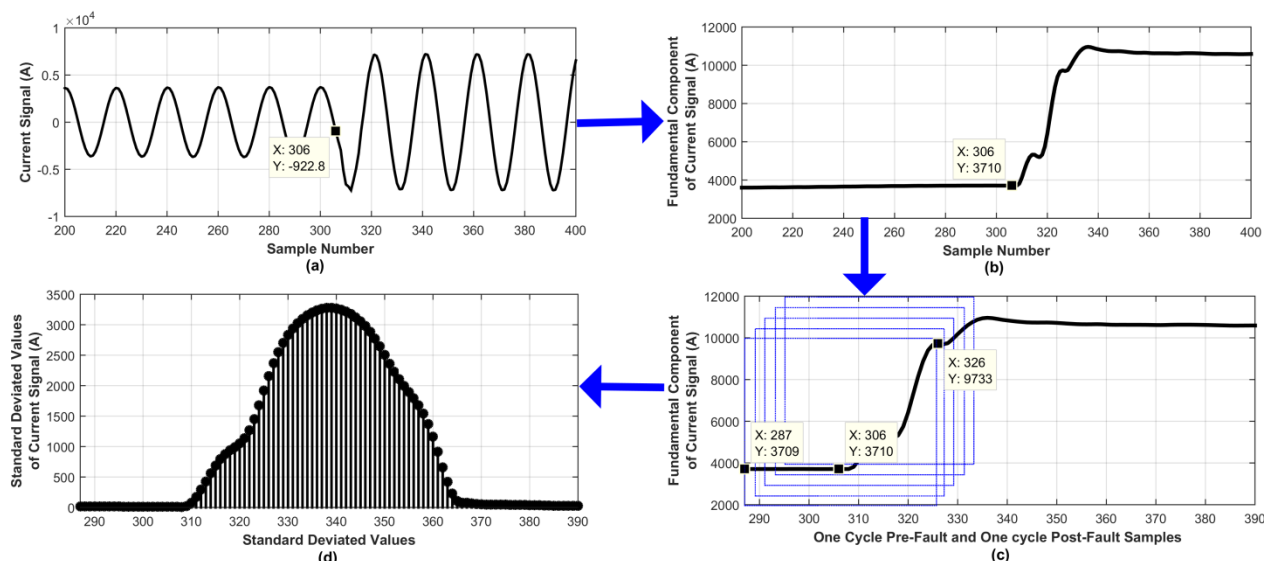


Fig. 3. Feature extraction during testing.

A similar process has been carried out to generate a test pattern for three-phase voltage and current signals, as well as for zero sequence current signals. Test results illustrating the different result for fault detection and classification have been discussed in proceeding section.

4. CASE STUDIES AND DISCUSSIONS

In this study, three machine four bus system as shown in Fig. 1 has been taken to evaluate various fault detection and classification task. Here two trained ANN, one for fault detection and one for fault classification has been simultaneously tested to evaluate their accuracy and reliability with a separate set of test data. The test data used in the performance evaluation have not been used during the training process of ANN. Table 2 shows the different conditions for which testing data set (4,64,640) have been generated. Trained ANN based fault detection and classification modules have been considered at bus 1. In the proceeding sections, the evaluation of the trained ANN-module has been carried out with the obtained time domain voltage and current signals at bus 1.

4.1. Performance in Case Ground Associated Shunt Faults

In case of unsymmetrical fault situations, FACTS devices provide equal three-phase compensation in each phase of the transmission line, consequentially healthy phases have overcompensation. This overcompensation of healthy phase increases the possibility of the incorrect phase selection in the conventional distance and current based relaying scheme. For an example at time $t = 0.255s$, and fault resistance of 0Ω phase to a ground fault has been simulated at near (3 km) from bus 1. Both the trained ANN

modules are tested in parallel and operating time is calculated. Fig. 4 depicts the test result in case of an AG internal fault. Fig. 4(a) and

Table 2. System parameter for testing set.

Parameter	Values
Fault Type	LG [AG, BG, CG]
	LLG [ABG, BCG, CAG]
	LL[AB, BC, CA]
	LLL[ABC, ABCG]
Fault Inception Angle [Degree]	0 - 360 (by step of 36)
Fault Resistance [Ohm]	0, 10, 20, 30, 40, 50, 60, 70, 80, 90, 100
Fault Location [km]	6-156 (by step of 6)
	7-154 (by step of 7)
UPFC References P [MW], Q [MVar], V [p.u.]	P = 1063; Q = 288; V = 1.04 P = 600; Q = 60; V = 1.04
STATCOM voltage reference [p.u.]	1.05; 1.03
SSSC voltage refence [p.u.]	0.1; -0.08

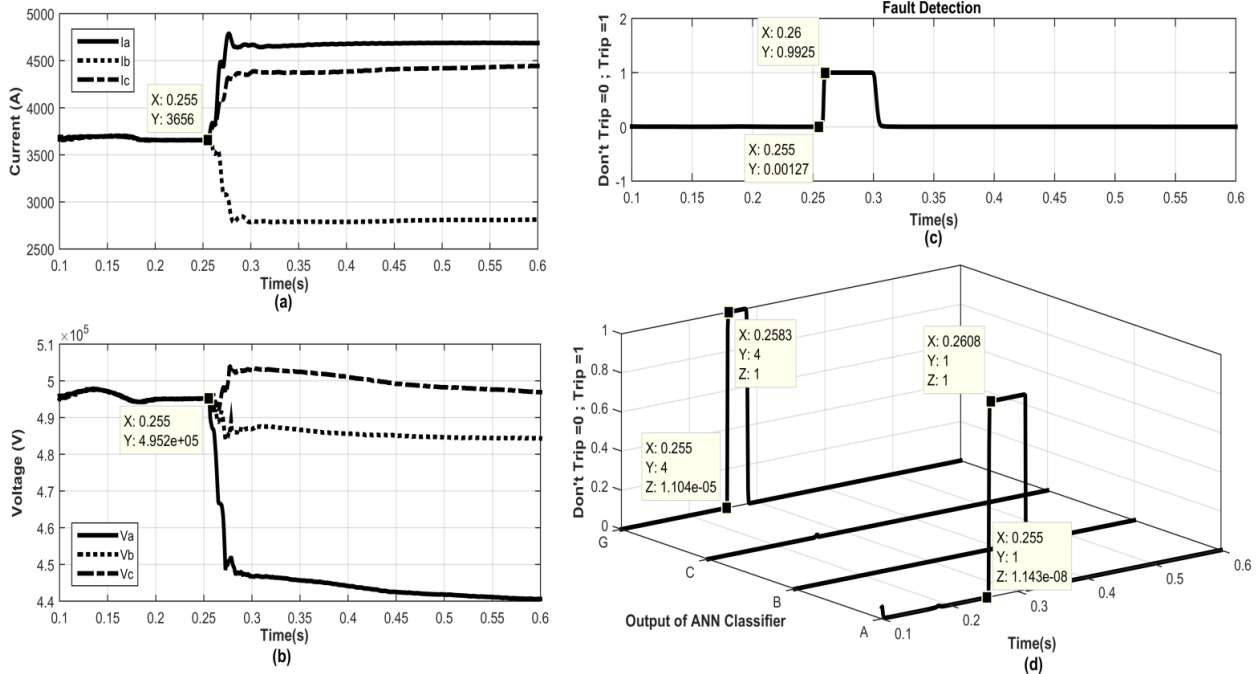


Fig. 4. Performance of ANN module (Near end) (a) Current Signals (b) Voltage Signals (c) Fault detection (d) Fault classification.

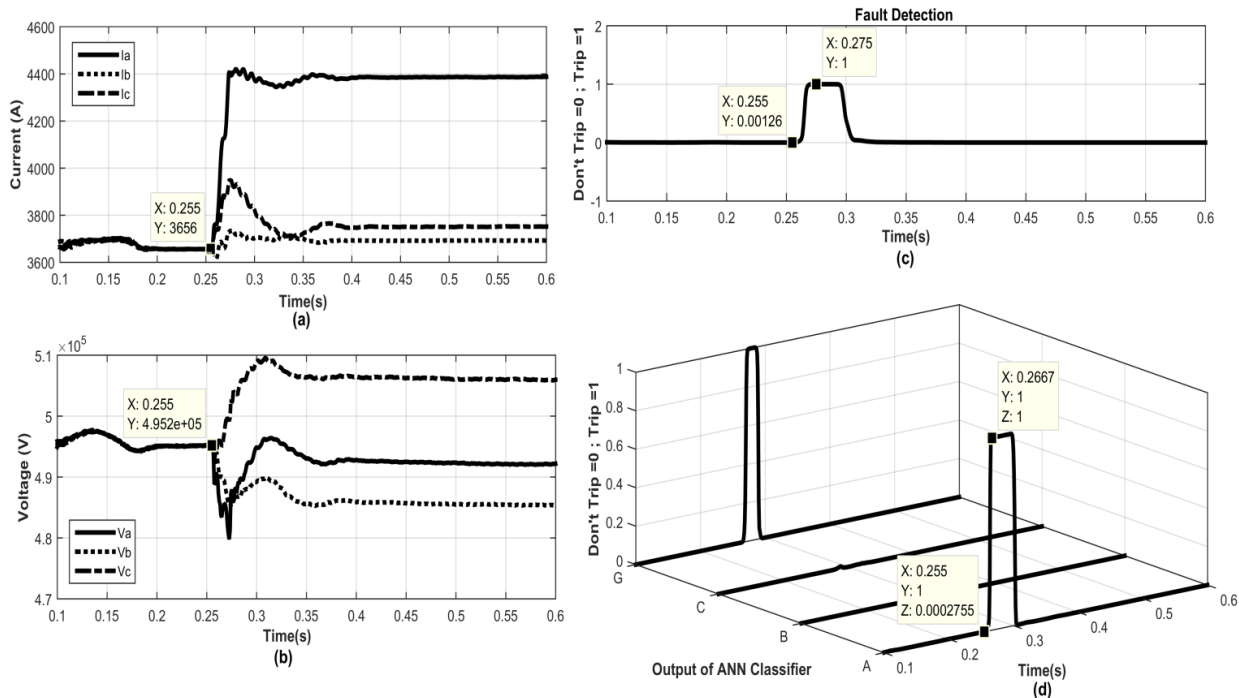


Fig. 5. Performance of ANN module (Far end) (a) Current Signals (b) Voltage Signals (c) Fault detection (d) Fault classification.

Fig. 4 (b) illustrates the fundamental component of current and voltage signals during AG fault condition. It can be observed from Fig. 4(a) and Fig. 4(b) that the current signal in phase A is increased drastically, simultaneously the voltage signal in phase A reduces. Sud-

den changes in current and voltage signals during shunt fault conditions outcomes a large positive value of standard deviation. It can be seen that ANN based fault detector module detected a fault within 5 ms for the fault associated near the relaying bus as shown in Fig.4

(c), simultaneously fault type is accurately classified as depicted in Fig 4(d). Fig. 4 enlightens for the fault detection and classification performance of the ANN-based scheme in case of fault near to the relaying location (bus 1). In the case of fault near to remote terminal (bus 3) with high resistance (100 Ω), the performance of the proposed scheme is exemplified in Fig. 5. From Fig. 5(a) and Fig. 5(b) it is clearly depicted that current and voltage signals are different in nature from Fig. 4(a) and Fig. 4(b) which leads the conventional distance relay to mal operate. However, in case of high resistance, fault case current signal is not significantly increased, compared to low resistance fault. Also, voltage signals are not much deviated during such

condition. From Fig. 5(c) and Fig. 5(d), it can be clearly observed that proposed scheme is able to detect the high resistance fault reliably and classify it correctly.

To validate the trained ANN module in different fault conditions, fault locations are randomly varied from bus 2 to bus 3, fault resistance varies from 0 Ω -100 Ω , and fault inception angle (FIA) from 0 $^\circ$ -360 $^\circ$. Reliability of the trained ANN is tested in terms of operating time, test result for a single line to ground (AG) fault are tabulated in Table 3. All the simulation studies have been performed in HP Z420 workstation with 4-GB RAM and Intel(R) Xeon 3.6-GHz processor.

Table 3. Fault detection time in case of AG fault with varying fault resistance and fault location.

Fault location/ Fault Resistance	Fault detection time (in ms)										
	0 Ω	10 Ω	20 Ω	30 Ω	40 Ω	50 Ω	60 Ω	70 Ω	80 Ω	90 Ω	100 Ω
7 km	4.2	4.2	4.2	5.0	5.0	5.8	6.7	7.5	8.3	8.3	9.2
14 km	4.2	4.2	5.0	5.0	5.8	5.8	6.7	7.5	8.3	9.2	9.2
21 km	4.2	4.2	5.0	5.0	5.8	6.7	6.7	7.5	8.3	9.2	10.0
28 km	4.2	4.2	5.0	5.0	5.8	6.7	7.5	8.3	8.3	9.2	10.0
35 km	4.2	5.0	5.0	5.8	5.8	6.7	7.5	8.3	9.2	9.2	10.0
42 km	4.2	5.0	5.0	5.8	5.8	6.7	7.5	8.3	9.2	10.0	10.0
49 km	4.2	5.0	5.0	5.8	6.7	7.5	7.5	8.3	9.2	10.0	10.8
56 km	5.0	5.0	5.8	5.8	6.7	7.5	8.3	9.2	9.2	10.0	10.8
63 km	5.0	5.0	5.8	5.8	6.7	7.5	8.3	9.2	10.0	10.0	10.8
70 km	5.0	5.0	5.8	6.7	6.7	7.5	8.3	9.2	10.0	10.8	10.8
77 km	5.0	5.0	5.8	6.7	7.5	8.3	9.2	9.2	10.0	10.8	11.7
84 km	5.0	5.0	5.8	6.7	7.5	8.3	9.2	10.0	10.8	10.8	11.7
91 km	5.0	5.8	5.8	6.7	7.5	8.3	9.2	10.0	10.8	10.8	11.7
98 km	5.0	5.8	6.7	6.7	7.5	8.3	9.2	10.0	10.8	10.8	11.7
105 km	5.0	5.8	6.7	7.5	8.3	9.2	10.0	10.8	10.8	11.7	11.7
112 km	5.0	5.8	6.7	7.5	8.3	9.2	10.0	10.8	11.7	12.5	13.3
119 km	5.0	5.8	6.7	7.5	8.3	9.2	10.0	10.8	11.7	12.5	13.3
126 km	5.0	5.8	6.7	8.3	9.2	10.0	10.8	11.7	12.5	13.3	14.2
133 km	5.8	5.8	6.7	8.3	9.2	10.0	10.8	11.7	12.5	13.3	14.2
140 km	5.8	5.8	6.7	8.3	9.2	10.0	10.8	11.7	13.3	14.2	15.0
147 km	5.8	5.8	7.5	8.3	9.2	10.8	11.7	12.5	13.3	14.2	15.8
154 km	5.8	5.8	7.5	8.3	10.0	10.8	11.7	12.5	13.3	15.0	15.8

Table 3 depicts that fault detection time is less than half cycle of fundamental frequency in most of the test cases whereas it can also be observed that fault detection time is within one fundamental frequency cycle in case of high resistance faults, which demonstrate the ability to fast detection of internal fault including high resistance fault.

4.2. Performance in case of Double Phase to Ground (LLG) and Double Phase Fault (LL)

To evaluate the performance of the proposed scheme for discrimination between LLG and LL fault, huge amount of test cases have been tested. For an example, a CA and CAG fault have been simulated at 157 km from bus 1 with the fault resistance and FIA of 100Ω and 108° , respectively. Fig. 6 graphically illustrates the test result, from Fig. 6(a) it could be seen that LL fault has been detected, meanwhile, LL fault has been classified successfully as depicted in Fig. 6(b). Fig. 6(b) and Fig. 6(d) clearly differentiate between CA and CAG fault.

Test results illustrating fault detection time for ABG fault with the fixed fault resistance of 20Ω and varying the fault location and fault inception angle are tabulated

in Table 4. From Table 4 it can be seen that fault detection is less than half cycle of fundamental frequency for most of the test cases, which demonstrated that sensitivity of the proposed scheme is not much deviated with the variation of fault inception angle.

4.3. Performance in the Presence of CT and CCVT

To analyse the performance of proposed scheme in case of signal distortion in presence of CT and CCVT, introduced error, each phase of the measuring point are connected with CT and CCVT on per phase basis at bus 1 of the test system as shown in Fig. 1. However, to show the error produced by this instrument, no compensation is used to reduce it. The CT's are rated 2000A/5A, 30 VA. When a fault occurs at zero fault inception angle; the current contains a high value of dc offset, this causes saturation of the CT and thus the current in the secondary of CT reduced considerably. Due to the presence of dc offset current in the measuring signals, instruments produce magnitude and phase angle error at the relay measuring point, consequently relay will mal-operate in such situation. Fig.7 (a,b) shows that voltage and current signals are in the primary and secondary sides of the instrument transformer.

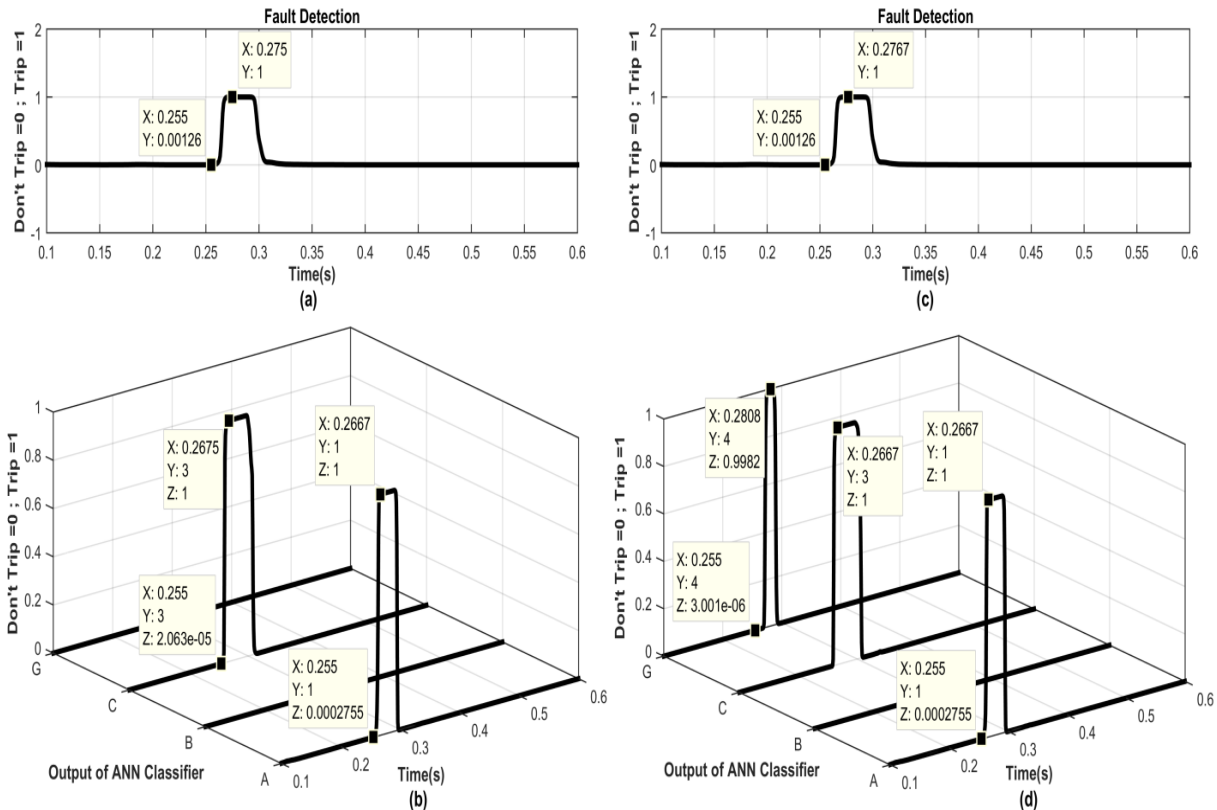


Fig. 6. Performance of ANN module (a) Fault detection (CA) (b) Fault classification (CA) (c) Fault detection (CAG) (d) Fault classification(CAG).

Table 4. Fault detection time in case of ABG fault with varying fault inception angle and fault location.

Fault location /Fault Inception Angle	Fault detection time (in ms)										
	0°	36°	72°	108°	144°	180°	216°	252°	288°	324°	360°
6 km	5.0	4.1	4.9	7.5	5.8	4.9	4.2	5.8	7.8	5.8	5.0
12 km	5.0	4.1	5.9	7.5	6.6	4.9	4.2	5.8	7.8	5.8	5.0
24 km	5.0	5.0	5.9	7.5	6.6	4.9	5.0	5.8	7.8	5.8	5.8
36 km	5.8	5.0	5.9	7.5	6.6	5.8	5.0	6.6	7.8	5.8	5.8
48 km	5.8	5.0	6.7	7.5	6.6	5.8	5.0	6.6	7.8	5.8	5.8
54 km	5.8	5.0	6.7	8.3	6.6	5.8	5.0	6.6	8.3	5.8	5.8
60 km	5.8	5.8	6.7	8.3	6.6	5.8	5.0	6.6	8.3	5.8	5.8
66 km	5.8	5.8	6.7	8.3	7.5	5.8	5.8	6.6	8.3	7.5	6.6
72 km	5.8	5.8	6.7	8.3	7.5	5.8	5.8	7.5	8.3	7.5	6.6
78 km	5.8	5.8	7.5	8.3	7.5	5.8	5.8	7.5	8.3	7.5	6.6
84 km	6.7	5.8	7.5	8.3	7.5	6.6	5.8	7.5	8.3	7.5	6.6
96 km	6.7	5.8	7.5	8.3	7.5	6.6	5.8	7.5	8.3	7.5	6.6
102 km	6.7	6.6	7.5	8.3	7.5	6.6	5.8	7.5	8.3	7.5	6.6
114 km	6.7	6.6	7.5	8.3	7.5	6.6	6.7	7.5	8.3	7.5	6.6
120 km	6.7	6.6	7.5	8.3	7.5	6.6	6.7	7.5	8.3	7.5	7.5
126 km	6.7	6.6	7.5	8.3	7.5	6.6	6.7	7.5	8.3	7.5	7.5
132 km	6.7	6.6	7.5	8.3	7.5	6.6	6.7	7.5	8.3	7.5	7.5
138 km	6.7	6.6	7.5	8.3	7.5	6.6	6.7	7.5	8.3	7.5	7.5
144 km	6.7	6.6	7.5	8.3	7.5	6.6	6.7	7.5	8.3	7.5	7.5
150 km	6.7	6.6	7.5	8.3	7.5	6.6	6.7	7.5	8.3	7.5	7.5
156 km	6.7	7.5	7.5	8.3	7.5	6.6	7.5	7.5	8.3	7.5	7.5

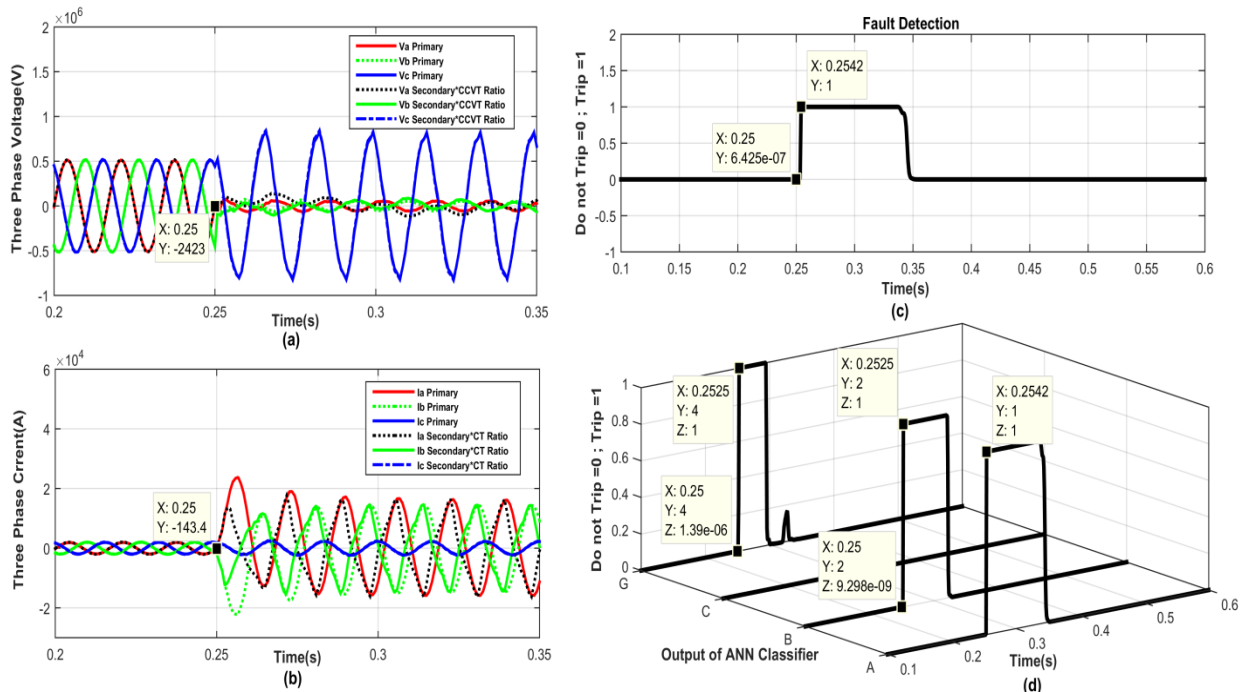


Fig. 7. Performance of the ANN module during CT and CCVT error. (a) Three phase voltage waveforms during an ABG fault at 0.25s with and without CCVT transients at bus 1.(c) Fault detection (d) Fault classification.

From Fig. 7 (a, b) it is clearly observed that the presence of the dc component in the primary fault signal makes the secondary side measured signals distorted. Consequently, measuring error introduces false operation of the relaying algorithms. The trained ANN has been tested in such situations and found that it detects and classifies the fault successfully as shown in Fig. 7 (c) and 7 (d).

4.4. Effect of Different Compensation Level

Whenever the fault occurred in the transmission line, the bus voltage changes suddenly and it affects the line flow. UPFC controller is designed to respond in case of measuring quantity changes from its reference quantity set by the utility. During fault condition measuring quantity changes drastically, consequently, it will affect the relaying measuring signals. When both STATCOM and SSSC operate together, the UPFC operates as a complete device and its function is to maintain bus voltage and regulate the power flow in the transmission line. Voltage and current signals received at relaying location are mostly influenced by the UPFC mode of operation as compared to standalone STATCOM and SSSC mode. The relaying algorithms also influenced with the different compensation levels or setting of the FACTS devices. Depending upon the different setting of the reference value of FACTS device it injects or absorbs the reactive power into the system which in turn deviates the characteristics of the voltage and current signals at relaying point. In this context testing signals have been generated in case of different compensation level as shown in Table 2, while the training patterns remain same as shown in Table 1. Obtained testing patterns have been tested with the trained ANN modules and outcome of test results proves that proposed scheme is not affected with the variation of compensation level.

4.5. Effect of Different Mode of Operation

UPFC has other possible modes, in this paper, the study has been concentrated on two individual modes of operation. In these two modes both the converters operate in the reactive power domain. The shunt converter operates as a standalone STATCOM and the series converter as SSSC. Under such condition, neither converter is capable of absorbing or generating real power so that only operation in the reactive power domain is possible [9]. In individual STATCOM and SSSC mode of operation, UPFC behaves as in particular shunt and series FACTS device respectively and the performance of the proposed protection scheme is discussed hereunder.

4.5.1. STATCOM mode of operation

When UPFC operates on STATCOM mode, it regulates the bus voltage at the point of connection. Whenever any shunt fault occurs, the bus voltage is altered. Hence, the associated shunt controller attempts to bring it to its reference value. To evaluate the performance during such conditions new testing sets with STATCOM compensator is generated. The corresponding conditions of new testing patterns are tabled in Table 2. Whereas the trained model is kept at before conditions as shown in Table 1. The trained model has been tested with the variation of different fault parameters. For example, a CG fault has been simulated in the test system with the variation of fault resistance and fault location. Evaluated test results with a STATCOM voltage reference value of 1.05pu are depicted in Table 5. The fault detection time in case of STATCOM mode of operation is within the one fundamental frequency cycle for all the test cases.

4.5.2. SSSC mode of operation

SSSC mode of operations provides voltage regulations by controlling effective line impedance. In this mode of operation, measuring signals are affected due to fast control action of the SSSC controller. To validate the performance of the proposed scheme during SSSC mode of operation, several fault simulations have been performed with the variation of fault location and fault resistance. Performance outcomes are tabulated in Table 6 that exemplifies adaptability of the proposed scheme, as fault detection time is less than half fundamental frequency cycle for most of the cases even for high resistance, fault detection time is less than one fundamental frequency cycle.

Test results in time domain during STATCOM and SSSC mode of operation is exemplified in Fig. 8. A CG and CAG fault was simulated at 49 km with 30 Ω fault resistance and 108 $^\circ$ FIA from bus 2 in both the STATCOM and SSSC operating mode. Fig. 8 (a, b) shows fault detection and classification results during STATCOM mode of operation, whereas Fig. 8 (c, d) depicts performance of fault detection and classification scheme during SSSC mode of operation. From Fig. 8 it can be observed that trained ANN modules for fault detection and classification show higher reliability during a different mode of operation. However, training patterns are different from the testing pattern.

Table 5. Fault detection time in case of CG fault with varying fault resistance and fault location (STATCOM).

Fault location /Fault Resistance	Fault detection time (in ms)										
	0 Ω	10 Ω	20 Ω	30 Ω	40 Ω	50 Ω	60 Ω	70 Ω	80 Ω	90 Ω	100 Ω
7 km	5.8	6.7	6.7	7.5	7.5	7.5	8.3	9.2	9.2	10.0	10.8
14 km	5.8	6.7	6.7	7.5	7.5	8.3	8.3	9.2	10.0	10.0	10.8
21 km	6.7	6.7	6.7	7.5	7.5	8.3	8.3	9.2	10.0	10.0	10.8
28 km	6.7	6.7	6.7	7.5	7.5	8.3	8.3	9.2	10.0	10.8	10.8
35 km	6.7	6.7	6.7	7.5	7.5	8.3	9.2	9.2	10.0	10.8	10.8
42 km	6.7	6.7	6.7	7.5	7.5	8.3	9.2	9.2	10.0	10.8	10.8
49 km	6.7	6.7	6.7	7.5	7.5	8.3	9.2	10.0	10.0	10.8	11.7
56 km	6.7	6.7	6.7	7.5	7.5	8.3	9.2	10.0	10.0	10.8	11.7
63 km	6.7	6.7	6.7	7.5	8.3	8.3	9.2	10.0	10.8	11.7	11.7
70 km	6.7	6.7	6.7	7.5	8.3	8.3	9.2	10.0	10.8	11.7	12.5
77 km	6.7	6.7	6.7	7.5	8.3	8.3	9.2	10.0	10.8	11.7	12.5
84 km	6.7	6.7	6.7	7.5	8.3	9.2	9.2	10.0	11.7	11.7	12.5
91 km	6.7	6.7	6.7	7.5	8.3	9.2	10.0	10.8	11.7	12.5	12.5
98 km	6.7	6.7	6.7	7.5	8.3	9.2	10.0	10.8	11.7	12.5	12.5
105 km	6.7	6.7	6.7	7.5	8.3	9.2	10.0	10.8	11.7	12.5	13.3
112 km	5.8	6.7	6.7	7.5	8.3	9.2	10.8	11.7	11.7	12.5	13.3
119 km	5.8	6.7	6.7	7.5	8.3	10.0	11.7	11.7	12.5	13.3	13.3
126 km	5.8	6.7	6.7	7.5	8.3	10.0	11.7	11.7	12.5	13.3	14.2
133 km	5.8	6.7	6.7	7.5	9.2	10.0	11.7	11.7	12.5	13.3	14.2
140 km	5.8	5.8	6.7	7.5	9.2	10.0	11.7	12.5	13.3	14.2	14.2
147 km	5.8	5.8	6.7	7.5	9.2	10.0	11.7	12.5	13.3	14.2	15.0
154 km	5.8	5.8	6.7	7.5	9.2	10.8	11.7	12.5	13.3	14.2	15.8

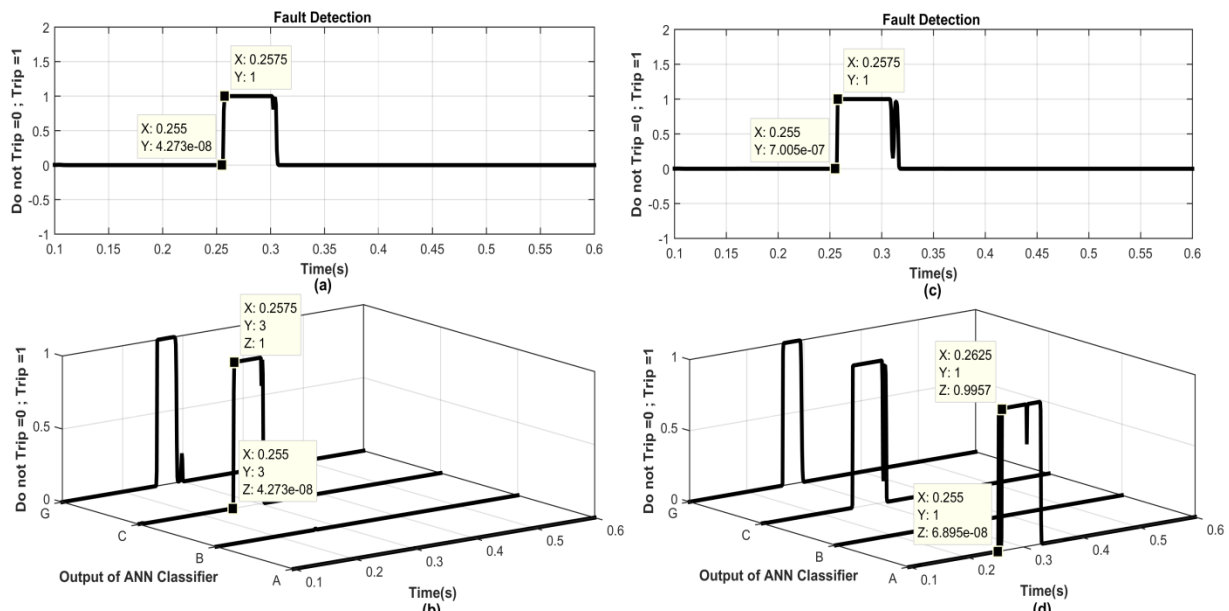


Fig. 8. Performance of ANN module during SSSC and STATCOM mode of operation (a) Fault detection (CG) (b) Fault classification (CG) (c) Fault detection (CAG) (d) Fault classification(CAG).

Table 6. Fault detection time in case of ACG fault with varying fault resistance and fault location (SSSC).

Fault location /Fault Resistance	Fault detection time (in ms)										
	0 Ω	10 Ω	20 Ω	30 Ω	40 Ω	50 Ω	60 Ω	70 Ω	80 Ω	90 Ω	100 Ω
7 km	3.3	4.2	4.2	4.2	5.0	5.0	5.0	5.8	5.8	6.7	6.7
14 km	4.2	4.2	4.2	4.2	5.0	5.0	5.8	5.8	6.7	6.7	7.5
21 km	4.2	4.2	4.2	5.0	5.0	5.0	5.8	5.8	6.7	6.7	7.5
28 km	4.2	4.2	4.2	5.0	5.0	5.8	5.8	5.8	6.7	7.5	7.5
35 km	4.2	4.2	5.0	5.0	5.0	5.8	5.8	6.7	6.7	7.5	7.5
42 km	4.2	4.2	5.0	5.0	5.0	5.8	5.8	6.7	6.7	7.5	8.3
49 km	4.2	4.2	5.0	5.0	5.8	5.8	6.7	6.7	7.5	7.5	8.3
56 km	4.2	5.0	5.0	5.0	5.8	5.8	6.7	6.7	7.5	7.5	8.3
63 km	4.2	5.0	5.0	5.0	5.8	5.8	6.7	6.7	7.5	8.3	8.3
70 km	4.2	5.0	5.0	5.8	5.8	6.7	6.7	7.5	7.5	8.3	9.2
77 km	5.0	5.0	5.0	5.8	5.8	6.7	6.7	7.5	8.3	8.3	9.2
84 km	5.0	5.0	5.0	5.8	5.8	6.7	7.5	7.5	8.3	8.3	9.2
91 km	5.0	5.0	5.8	5.8	6.7	6.7	7.5	7.5	8.3	9.2	9.2
98 km	5.0	5.0	5.8	5.8	6.7	6.7	7.5	8.3	8.3	9.2	10.0
105 km	5.0	5.0	5.8	5.8	6.7	7.5	7.5	8.3	9.2	9.2	10.0
112 km	5.0	5.0	5.8	5.8	6.7	7.5	7.5	8.3	9.2	10.0	10.0
119 km	5.0	5.0	5.8	6.7	6.7	7.5	8.3	8.3	9.2	10.0	10.8
126 km	5.0	5.8	5.8	6.7	6.7	7.5	8.3	9.2	9.2	10.0	10.8
133 km	5.0	5.8	5.8	6.7	7.5	7.5	8.3	9.2	10.0	10.8	10.8
140 km	5.0	5.8	5.8	6.7	7.5	8.3	8.3	9.2	10.0	10.8	11.7
147 km	5.0	5.8	5.8	6.7	7.5	8.3	9.2	10.0	10.0	10.8	11.7
154 km	5.0	5.8	5.8	6.7	7.5	8.3	9.2	10.0	10.8	11.7	12.5

5. CONCLUSION

ANN-based Fault detection and classification scheme is presented in this paper for transmission line compensated with UPFC device. The advantage of the proposed scheme over conventional scheme is that it has a reach setting up to 99 % of the line length. It has the ability to classify all the shunt fault types accurately. Rigorous simulation studies bring-outs its superiority in case of large variation in different fault type, fault inception angle, fault resistance, CT saturation and CCVT transients. Reliability of the scheme is validated in the different mode of the UPFC operation, various compensation levels or reference values. Moreover, in all the simulation cases, fault classification accuracy is 98.9%.

REFERENCES

- [1] Hingorani N. G. And Gyugyi L., "Understanding FACTS Concept and Technology of Flexible AC Transmission System", Wiley IEEE Press, 2000.
- [2] X. Zhou, H. Wang, R. K. Aggarwal, and P. Beaumont, "Performance Evaluation of a Distance Relay as Applied to a Transmission System with UPFC," *IEEE Trans. Power Deliv.*, Vol. 21, No. 3, pp. 1137–1147, 2006.
- [3] F. A. Albasri, T. S. Sidhu, and R. K. Varma, "Performance Comparison of Distance Protection Schemes for Shunt-FACTS Compensated Transmission Lines," *IEEE Trans. Power Deliv.*, Vol. 22, No. 4, pp. 2116–2125, 2007.
- [4] M. Khederzadeh and A. Ghorbani, "Impact of VSC-based Multiline FACTS Controllers on Distance Protection of Transmission Lines," *IEEE Trans. Power Deliv.*, vVol. 27, No. 1, pp. 32–39, 2012.
- [5] Z. Moravej, M. Pazoki, and M. Khederzadeh, "Impact of UPFC on power swing characteristic and distance relay behavior," *IEEE Trans. Power Deliv.*, Vol. 29, No. 1, pp. 261–268, 2014.
- [6] Kumar B., Yadav A., "Backup Protection Scheme for Transmission Line Compensated with UPFC during High Impedance Faults and Dynamic Situations," *IET Sci. Meas. Technol.*, Vol. 11, No. 6, pp. 703–712, 2017.
- [7] M. C. R. Paz, R. C. Leborgne, and A. S. Bretas, "Adaptive Ground Distance Protection for UPFC Compensated Transmission Lines: A Formulation Considering The Fault Resistance Effect," *Int. J. Electr. Power Energy Syst.*, Vol. 73, pp. 124–131, 2015.

- [8] H. Mehrjerdi and A. Ghorbani, "Adaptive Algorithm for Transmission Line Protection in the Presence of UPFC," *Int. J. Electr. Power Energy Syst.*, Vol. 91, pp. 10–19, 2017.
- [9] C. D. Schauder *et al.*, "Operation of the Unified Power Flow Controller (UPFC) under practical constraints," *IEEE Trans. Power Deliv.*, Vol. 13, No. 2, pp. 630–637, 1998.
- [10] P. K. Dash, A. K. Pradhan, and G. Panda, "Distance Protection in the Presence of Unified Power Flow Controller," *Electr. Power Syst. Res.*, Vol. 54, No. 3, pp. 189–198, 2000.
- [11] S. R. Samantaray, "Decision Tree-Based Fault Zone Identification and Fault Classification in Flexible AC Transmissions-Based Transmission Line," *IET Gener. Transm. Distrib.*, Vol. 3, No. 5, p. 425, 2009.
- [12] S. R. Samantaray, "A Data-Mining Model for Protection of Facts-Based Transmission Line," *IEEE Trans. Power Deliv.*, Vol. 28, No. 2, pp. 612–618, 2013.
- [13] A. Manori, M. Tripathy, and H. O. Gupta, "SVM based Zonal Setting of Mho Relay for Shunt Compensated Transmission Line," *Int. J. Electr. Power Energy Syst.*, Vol. 78, pp. 422–428, 2016.
- [14] L. Tripathy, M. K. Jena, and S. R. Samantaray, "Decision Tree-Induced Fuzzy Rule-Based Differential Relaying for Transmission Line Including Unified Power Flow Controller and Wind-Farms," *IET Gener. Transm. Distrib.*, Vol. 8, No. 12, pp. 2144–2152, 2014.
- [15] R. Dubey, S. R. Samantaray, B. K. Panigrahi, and Vijendran G. Venkoparao, "Extreme Learning Machine Based Adaptive Distance Relaying Scheme for Static Synchronous Series Compensator Based Transmission Lines," *Electr. Power comp.and syst.* Vol. 44, No. 2, pp. 219-232 December, 2015.
- [16] Z. Moravej, S. Member, M. Pazoki, M. Khederzadeh, and S. Member, "New Pattern-Recognition Method for Fault Analysis in Transmission Line With UPFC," Vol. 30, No. 3, pp. 1231–1242, 2015.
- [17] A. Yadav and A. Swetapadma, "Electrical Power and Energy Systems A Single Ended Directional Fault Section Identifier and Fault Locator For Double Circuit Transmission Lines using Combined Wavelet and ANN Approach," Vol. 69, pp. 27–33, 2015.
- [18] A. Yadav and A. Swetapadma, "Improved First Zone Reach Setting of Artificial Neural Network-Based Directional Relay for Protection of Double Circuit Transmission Lines," *IET Gener. Transm. Distrib.*, Vol. 8, No. 3 pp. 373–388, 2014.
- [19] SimPower Systems Toolbox ver. 8.1, for use with Simulink, User's Guide. The Math Works, Inc., 2013a.